Cellulose (2008) 15:425–433
DOI 10.1007/s10570-007-9184-2

Rheological properties of microfibrillar suspension of TEMPO-oxidized pulp

Elsa Lasseuguette · Denis Roux · Yoshiharu Nishiyama

Received: 25 May 2007 / Accepted: 25 September 2007 / Published online: 27 October 2007

Abstract The rheology of cellulose microfibril suspensions from TEMPO-oxidized pulp was investigated. The suspension showed a pseudo-plastic and thixotropic behavior, slowly evolving with time under a given shear rate. The viscosity was proportional to the concentration up to the critical concentration of 0.23%. Above it, the viscosity followed a power law with exponents from 2 to 6 depending on the shear rate, and the system showed shear thinning behavior and behaved gel-like. Below this concentration, the system was more Newtonian. Birefringence measurement of 0.44% and 0.78% suspension showed that microfibrils alignment saturated at a small shear rate with a Herman's orientation parameter below 0.65 probably due to the interconnection of microfibrils.

Keywords Cellulose microfibrils · TEMPO oxidation · Rheology

Introduction

Well-dispersed cellulose fibrils that are nano-meters in lateral size and undefined length over micrometers, have various actual or potential applications such as:

- Thickener, emulsion stabilizer (Turbak et al. 1983) related to their rheological properties,
- Filler retention aid in paper making (Hioki et al. 1995),
- Composite materials (Zimmermann et al. 2004; Nakagaito and Yano 2004, 2005), due to their morphology and large surface area (Herrick et al. 1983), and high mechanical performances.

The nano-metric size has also another advantage of limiting the scattering of visible light during elaboration of transparent materials (Yano et al. 2005).

Microfibrillated cellulose (MFC) and bacterial cellulose are the most studied in view of such applications since they can be easily obtained in large quantity. MFC is mostly obtained by mechanical homogenization of secondary wall of fibers such as wool pulp. It is also reported that primary wall with charged polysaccharide matrix such as sugar beet pulps give better dispersion of microfibrils (Dinand et al. 1996, 1999). Bacterial cellulose, produced by some species of *Acetobacter* as extracellular polysaccharide, is natively occurring as a sparse network of cellulose microfibrils about 10 nm thick and

---

E. Lasseuguette · Y. Nishiyama (✉)
Centre de Recherche sur les Macromolécules Végétales, CNRS/UJF/ICMG, BP 53, 38041 Grenoble Cedex 9, France
e-mail: yoshi@cermav.cnrs.fr

D. Roux
Laboratoire de Rhéologie, UMR 5520 UJF/CNRS/INPG, BP 53, 38041 Grenoble Cedex 9, France

provides an attractive alternative if the fermentation cost could be drastically decreased. Cellulose microfibrils grafted with charged polymer also disperse in water without harsh mechanical impacts and attain a maximum viscosity when the grafting level is just enough to individualize the microfibril (Lepoutre and Robertson 1974). Those cellulose suspensions exhibit thixotropic and shear thinning behavior, and in general the finer the fibrils, the higher the viscosity for a given concentration.

Other examples of microfibrils dispersion can be found in certain seed mucilage and related system (Vian et al. 1994; Azuma and Sakamoto 2003). In those systems each microfibril is covered with partially charged polysaccharides that keeps the microfibrils from collapsing on to each other and extensively swells with water. Although small in quantity, such systems illustrate the potential functionalities of dispersed microfibrils.

Recently, we found that above a certain oxidation level of primary alcohol, even the tightly wound wood pulp or cotton microfibrils could be easily dispersed as individual microfibrils in water, by a simple mechanical treatment with a Waring-Blendor (Saito et al. 2006). The morphological aspects of such microfibrils were detailed in a recent study (Saito et al. 2007). The suspension was very viscous and showed permanent birefringence even at a concentration of 0.1%. Thus we further studied the rheological behavior of the microfibrillar suspension obtained by mechanical treatment of TEMPO oxidized native cellulose, using steady state as well as dynamic and rheo-optical measurements.

Experimental section

Materials

Never dried bleached sulfite pulp from Pinus pinaster with 29% solid content was shipped from Tembec Tartas pulping factory and stored at 4 °C before use. Other chemical products were purchased from Sigma Aldrich and used without purification.

Preparation of microfibrils

The method to prepare microfibrils suspensions and its morphological aspects are reported elsewhere (Saito et al. 2006). In short, the never dried cellulose (5 g of cellulose content) was suspended in water (500 mL), with TEMPO (0.23 g, 0.05 eq) and sodium bromide (1.3 g, 0.5 eq). A solution of 13% NaOCl was added dropwise to the mixture at room temperature under gentle stirring. The pH was maintained at 10.5 by adding 0.5 M NaOH. When no more decrease of pH was observed, the reaction is stopped by an addition of methanol (60 mL). The TEMPO oxidized product was thoroughly washed with distilled water by filtration and stored at 4 °C.

The slurries of oxidized pulp thus obtained were treated with a Waring-Blendor with a starting solid content of 4%. The suspension thus obtained (solid content about 0.1%) was centrifuged at 12,000 g in order to remove large particles (about 5% of the solid material).

Then, the suspension was concentrated by dialysis against a concentrated high molecular weight polyethylene glycol solution and dispersed again by an ultrasonic treatment using SONIFIER B12 (Branson Sonic Power Company). Samples with lower concentrations were prepared by diluting the high concentrated suspension with distilled water and dispersed by sonication.

Rheological experiments were achieved at room temperature using rheometers *TA instruments* (AR1000, ARES) operated with cone-and-plate geometries (cone angle: 4°, diameter: 2, 4 and 6 cm depending on the sample viscosity). The experiments are done with stepwise increment of shear rate or shear stress in order to follow the evolution of viscosity, and with continuous shear rate sweeps to confirm the reproducibility.

The measurements of modules G' and G'' were made with an applied strain between 5 and 15% depending on the concentration, in order to stay in the linear viscoelasticity range and ensure a measurable signal. At higher strain the G' and G'' tended to decrease.

To avoid water evaporation, a small amount of silicone oil was placed on the periphery of the solutions, or an evaporation blocker was used.

Rheo-optical experiments were performed with a photo-elastic modulator (PEM) developed by Fuller (1995) associated to a parallel-plate geometry with a fixed gap of 1.04 mm. A HeNe laser light of a wavelength $\lambda = 632$ nm was used as the incident beam. Transmitted signals are collected on a detector and go through two amplifiers-filters referenced to the frequency of modulation, ω, of the PEM. The first amplifier-filter generates a signal $I_1(\omega)$ whereas the second amplifier-filter generates a signal $I_2(\omega)$, which are the first and second harmonic of the collected signal. The phase difference ϕ between reference and transmitted signal is given by

$$\phi = \arcsin\left\{\frac{\sqrt{(AI_1)^2 + (BI_2)^2}}{I_0}\right\}$$

where A and B are two calibrated constants. The orientation angle is equal to

$$\theta = \arctan\left(\frac{-AI_1}{BI_2}\right),$$

and the birefringence is given by

$$\Delta n = -\frac{\lambda \cdot \phi}{2\pi \cdot h},$$

where h is the thickness of the sample, defined here by the gap (1.04 mm). In this configuration the direction of the flow is given for an orientation angle of $\theta = 45°$.

As was described elsewhere (Saito et al. 2006), the oxidized pulp suspension significantly increases its viscosity during the Waring-Blendor treatment to a point where it gels and the blade turns in air. To continue the treatment, water has to be added progressively. Figure 1 shows the shear rate dependence of the pulp suspension during the mechanical treatment when the solid content is 0.4%. The four lines are from different aliquots taken from the suspension during the treatment, showing increasing viscosity with increasing treatment time. Similar behavior is seen when wood pulp are mechanically treated with high-pressure using a Gaulin type homogenizer, in which case the fibrils become finer during the treatment. The viscosity at 100 s^{-1} of the 0.4% suspension from oxidized pulp at the end of the Waring-Blendor treatment is about the same as 2% MFC from pine sulfite pulp treated with 10 homogenizing passes at 55 MPa, reaching its maximum viscosity.

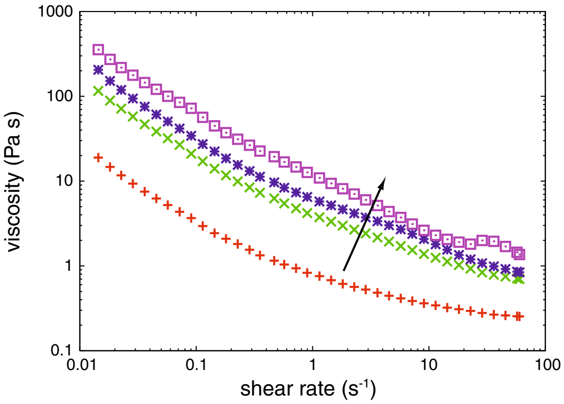

Fig. 1 Viscosity of 0.4% oxidized cellulose fibers suspension during the Waring-Blendor treatment as a function of shear rate. The arrow shows the treatment time increase

The system shows a shear thinning behavior but to a less extent compared to MFC and is more similar to the behavior of cellulose whiskers (sulfuric acid hydrolyzed cellulose of highly crystalline cellulose) suspensions (Bercea and Navard 2000). This is probably due to the polyanionic nature of the TEMPO oxidized microfibrils. Indeed, when pH is lowered by adding HCl, the microfibrillar suspensions become translucent gels, probably because all the carboxyl groups become protonated and loose their charge. Thus at higher pH the fluidity is ensured by the electrostatic repulsion between microfibrils.

When observes under optical microscope, the system contains both apparently intact pulp fibers and microfibrils that can be only observed with electron microscope, with very few intermediate fragments. During the treatment, the number of intact fibers decreases, and thus the concentration of microfibril increases. The increase of viscosity is probably related to the increase of microfibrils concentration, since the intact fibers are just suspended in the system without any interconnection between them.

Suspension that is completely transparent to naked eyes can be prepared either by continuing the treatment up to the dilution of 0.1%, or by sonication at higher concentration followed by removal of large particles by centrifugation. However, when we increase the concentration either by evaporation or by dialysis against concentrated polyethylene glycol, we observe whitening and gelation, and sonication is needed to re-disperse the system. In this case there is a large decrease in viscosity especially at low shear rate and the viscosity becomes less dependent on the shear rate (Fig. 2), although the morphology is undistinguishable with electron microscope (data not shown). The sonicated suspension also shows less thixotropic behavior in contrast to the non-sonicated suspension.

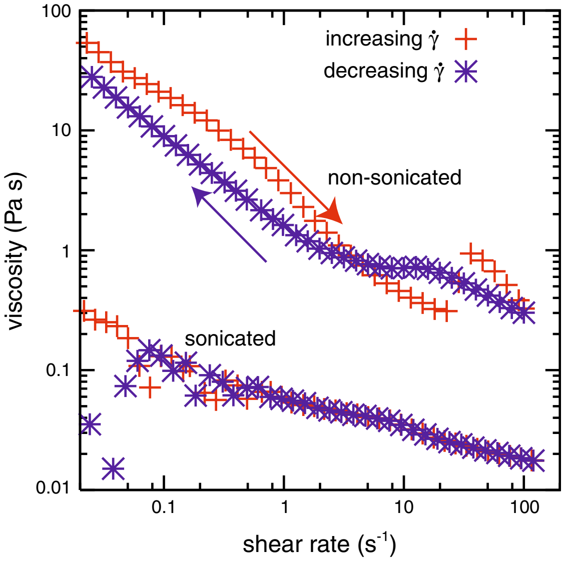

Fig. 2 Viscosity of 0.28% oxidized microfibril suspension before and after sonication as a function of the shear rate. The arrow shows whether the experiment was done with increasing or decreasing shear rate

Before sonication, the microfibrils probably create networks through sparse binary associations that can be disrupted by an ultrasound treatment. The suspensions, when left at 5 °C over weeks, also show apparent increase in viscosity. In the following, to investigate the rheological behavior of the microfibril suspension, we systematically apply sonication prior to all measurements.

Figure 3a shows the evolution of viscosity as a function of time after shear rate was incremented from 0 to 0.1 s^{-1}, from 0.1 to 0.5 s^{-1}, from 0.5 to 1 s^{-1} and from 1 to 10 s^{-1}. The viscosity rises rapidly at first and achieves a maximum at a deformation of around 1, and then slowly decreases. The viscosity continues to decrease in most cases well above 200 s, but then decreases almost linearly with the logarithm of time. Thus the system continues to slowly evolve over a very long period of time. On the other hand when we performed the measurement with several cycles of increasing and decreasing shear rate, the shear rate dependence of viscosity is reproducible from the second cycle (Fig. 3b). We can explain this phenomenon by difference in kinetics of break down and build up of flocks. Part of the aggregation would break up relatively rapidly during the first cycle whereas their formation at still is very slow at low shear rate masking the thixotropy loop after second cycle. This kind of behavior is currently observed with various colloidal suspensions (Barnes 1997). In the following, values at 200 s are taken for practical convenience.

The shear rate dependency of the shear stress and shear viscosity of the microfibrils suspension with different cellulose concentration is shown in Fig. 4. In the measured shear rate range, all suspensions follow the power law,

$$\sigma = \mathrm{K}{*}\dot{\gamma}^{n},$$

where K is the consistency coefficient and n is the flow behavior index. The *n* equal to unity indicates a Newtonian fluid, and *n* smaller than 1 indicates a pseudo-plastic behavior.

A clear tendency can be seen where *n* tends to the unit at lower concentration, and decreases with increasing concentration (Table 1).

The shear thinning is superior for higher concentration. At 1%, the viscosity is inversely proportional to the shear rate, whereas 0.15% suspension has an almost constant viscosity over the whole shear rate from 0.1 to 100 s^{-1}. This tendency and the absolute

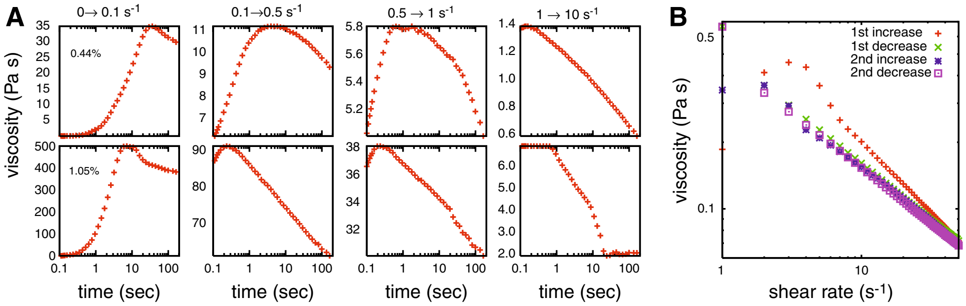

Fig. 3 (**a**) Viscosity as a function of time after the stepwise increment of the shear rate was applied to the 0.44% and 1.05% microfibril suspension. (**b**) Viscosity versus shear rate of the suspension subjected to cycles for 0.13% microfibril suspension

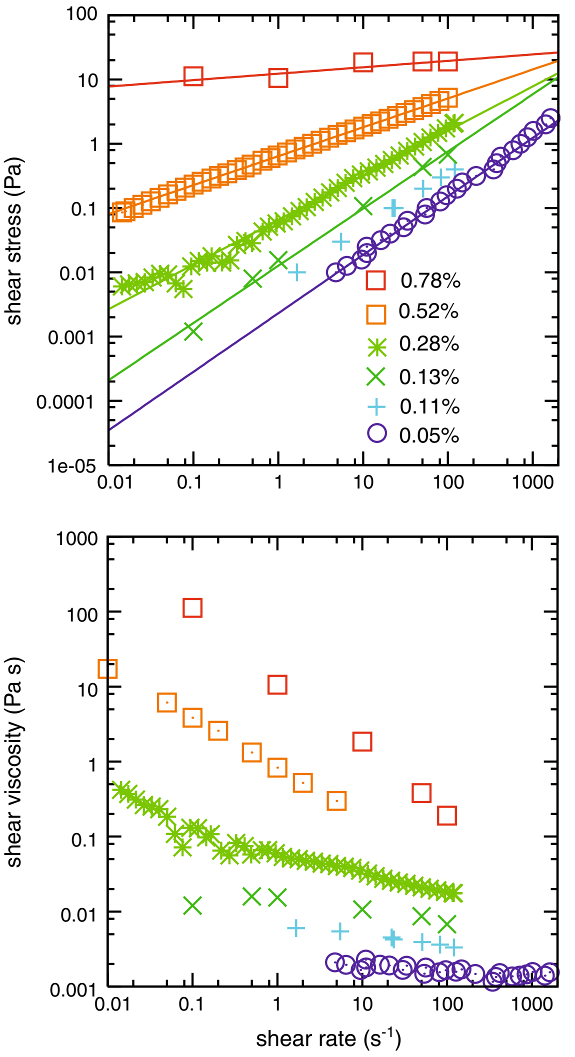

Fig. 4 Variation of shear stress and viscosity as a function of the shear rate for different concentrations of oxidized microfibrils. The lines are guide to the data with power law

value of viscosity at concentration lower than 0.2% are similar to what has been observed on cellulose whiskers suspension. Above 0.5%, the viscosity at low shear rate increases rapidly and the shear thinning behavior is more pronounced than whiskers suspension (Fig. 4).

Table 1 Power law parameters for microfibrils suspension at several concentrations

Concentration (%)	K	*n*
0.053	0.0023	0.9
0.11	0.008	0.89
0.13	0.0126	0.89
0.28	0.065	0.69
0.52	0.65	0.45
0.78	12.31	0.1

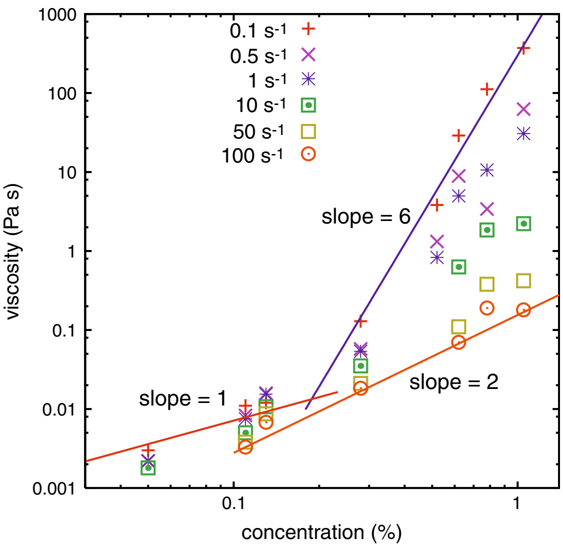

Fig. 5 Viscosity as a function of cellulose concentration at different shear rates

We cannot measure the viscosity precisely enough at low concentration—low shear rate regime because of the sensitivity of rheometer. Since the viscosity follows power law with respect to the shear rate, zero-shear viscosity cannot be extrapolated from the experiment. However, when viscosity is plotted as a function of concentration, there is clearly a flexion point for low shear rate at around 0.2% of cellulose concentration. Although the value for slow shear rate and small concentration suffer experimental limitation, with a shear rate of 0.1 s^{-1}, a straight line with a slope 1 can be drawn up to this critical concentration c*, and follows a power law with an exponent 6 above c* (Fig. 5). This is similar to polymer solution which in the dilute regime, zero shear rate specific viscosity is almost proportional to the concentration in the semi-dilute regime, and follows a power law with exponent above 3. The critical concentration in flexible polymers corresponds to the overlap concentration related to the radius of gyration and molecular weight (Doi and Edwards 1986). However, it seems to be unrealistic to measure the molecular weight and radius of gyration since the length scale is much larger than classical polymers.

The TEM observation shows kinked microfibrils with each segment between the kinks extending over the range of 100 nm (see Saito et al. 2006). Thus we consider a simple geometric model supposing that the system consists of microgels held by tetragonal arrangement of microfibrils. The volume v of a tetragonal with a side length of h is

$$v = \frac{h^3}{6\sqrt{2}}$$

whereas the total side length is $6h$. Each side can be shared by 8 neighboring tetragons, so the microfibril length l needed to occupy the space is $6/8h$. Using the cross-section area of the microfibrils, a, volume fraction of the microfibril ϕ necessary to fill the whole space will the gel can be expressed as

$$\phi = \frac{l}{v} = \frac{6ha}{8}\frac{6\sqrt{2}}{h^3} = 6.36\frac{a}{h^2}.$$

Assuming a squared cross section and a width of 3 nm, and the crystal density of cellulose, 1.6 g/cm^3, the side length with respect to concentration (weight %), c, will be

$$h = 7.56\sqrt{100/c}$$

with c = 0.23%, h is about 160 nm corresponding to the length scale between the kinks observed with electron microscopy, and the leveling off degree of polymerization by hydrolysis that is considered to be a distance between disordered region present in the microfibrils in higher plants (Nishiyama et al 2003).

Frequency dependence of the G′ and G″ is shown in Fig. 6. It can be seen that the G′ and G″ are almost parallel for the whole concentration and frequency range investigated. The storage modulus, G′, increases much more rapidly with concentration, and is greater than the loss modulus (G″) above 0.5% cellulose. It indicates a gel-like behavior, in the time scale shorter than seconds. The elastic contribution increases rapidly with concentration, which is in agreement with the steep increase of viscosity in the steady state.

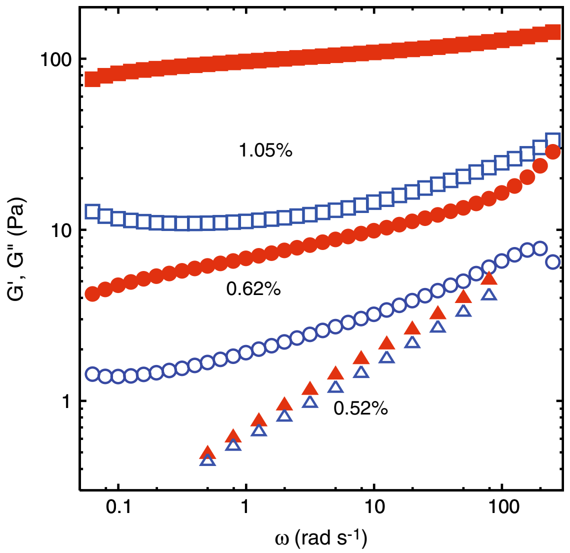

Fig. 6 Storage modulus and loss modulus of oxidized microfibril suspension as a function of angular frequency. Filled symbols correspond to G′ and open symbols correspond to G″

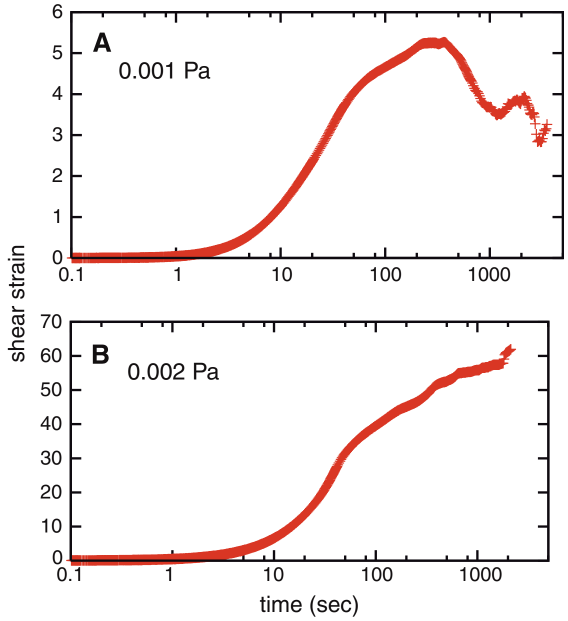

Fig. 7 Strain as a function of time under shear stress of 0.001 Pa and 0.002 Pa for 0.53% microfibril suspension

Figure 7a and 7b shows the shear strain as a function of time for applied stress of 0.001 and 0.002 Pa respectively for a 0.11% microfibril suspension. At shear stress of 0.001 Pa, the system slowly deforms up to a strain of 3–4 over 100 s, and stabilizes, behaving as an elastic gel. At 0.002 Pa on the other hand, the system continues to flow at an almost constant shear rate. With higher shear stress or lower concentration, the behavior is similar to the Fig. 7b. This concentration of 0.11% is lower than the critical concentration estimated from concentration dependence of viscosity. This discrepancy probably comes from the fact that in the imposed stress experiments no microfibrillar association is disrupted, whereas with imposed shear rate, the viscosity reflects the property after disruption of certain structure.

Figure 8 shows the birefringence of suspensions at two different concentrations as a function of shear rate. The birefringence can be directly related to the orientation of the microfibrils assuming the birefringence of the surface oxidized microfibril is the same as native cellulose crystals. The crystal birefringence of cellulose (parallel and perpendicular to the chain direction) has been measured to be 0.08 (Krishna et al. 1968). The form birefringence according to Wiener (1912) formula is,

$$n_e^2 - n_o^2 = \left[\frac{V_1 V_2 (n_1^2 - n_2^2)^2}{V_2 n_1^2 + (1 + V_1) n_2^2}\right],$$

where n_e and n_o is extraordinary and ordinary refractive index, V_1 and V_2 is the volume fraction of rods and matrix, n_1 and n_2 are the refractive index of the rods and matrix respectively. Since our suspension is very dilute, $V_2 \sim 1$ and $V_1 \ll 1$. The average refractive index should be close to water so the birefringence per volume fraction of rods can be approximated by

$$\frac{n_e - n_o}{V_1} \approx \left[\frac{(n_1^2 - n_2^2)^2}{2n\left(n_1^2 + n_2^2\right)}\right].$$

Using refractive index of water 1.33, and the average refractive index of cellulose 1.56, the form birefringence will be 0.043. Thus, with perfect orientation of microfibrils perpendicular to the laser

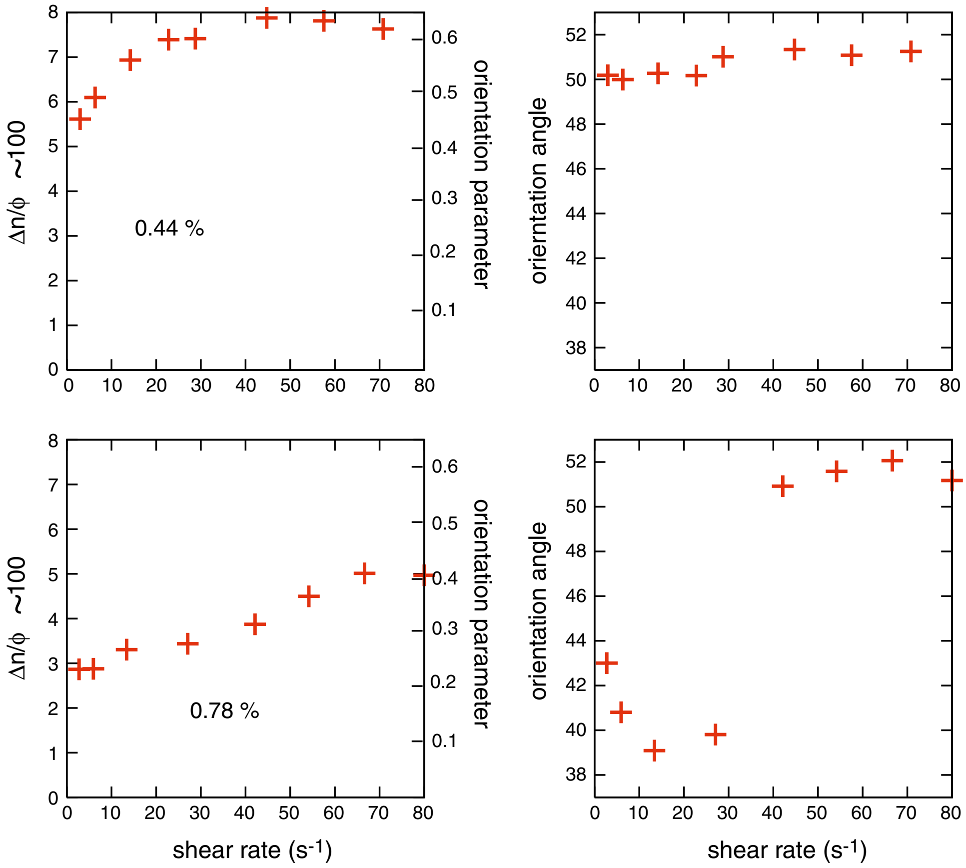

Fig. 8 Normalized birefringence and orientation angle, with respect to the analyzer, of 0.44 and 0.78% microfibril suspension as a function of shear rate

light, the birefringence is expected to be 0.123 per volume fraction of cellulose. The inclination angle χ of the microfibrils with respect to the shear plate cannot be measured with the present geometry. However, birefringence measurement on acid hydrolyzed cellulose using double cylinder geometry as well as theoretical calculation on rods suggests that the inclination angle should be very small (<5°) (Marchessault et al 1961). In this case the effect of inclination on the measured birefringence is negligible and the Herman's orientation parameter can be approximated by the ratio of observed birefringence and theoretical birefringence of perfect orientation.

The orientation parameter of 0.44% suspension seems to attain a maximum value of 0.65 at a shear rate around 40 s^{-1} and the orientation angle is almost parallel to the flow direction. The deviation from 45° of orientation angle is within the calibration error. On the other hand the birefringence of 0.78% solution continues to increase over the whole experimental range. A drastic change in orientation angle can be seen between 30 and 40 s^{-1} indicating that an important structural change, such as disruption of microgels, occurs due to the shear stress.

Conclusion

The cellulose microfibrils suspensions obtained by a combination of TEMPO mediated oxidation and mechanical treatment of native cellulose was found to be a system that slowly evolves with time under shear stress. Nevertheless an appropriate procedure allowed us to characterize its rheological properties.

The system showed shear thinning behavior without apparent plateau. At low concentration, the viscosity increased linearly with concentration, whereas at higher concentration the viscosity followed a power law with the exponent between 2 and 6, which decreased with shear rate.

The system showed a gel-like behavior with a clear yield stress showing an elastic behavior even at a concentration as low as 0.1%.

Birefringence measurement allowed us to follow the orientation of microfibrils under shear flow. At high concentration, high shear stress was required to obtain the alignment of fibrils.

References

Azuma J, Sakamoto M (2003) Cellulosic hydrocolloid system present in seed of plants. Trends Glycosci Glycotechnol 15:1–14

Barnes HA (1997) Thixotropy—a review. J Non-Newtonian Fluid Mech 70:1–33

Bercea M, Navard P (2000) Shear dynamics of aqueous suspensions of cellulose whiskers. Macromolecules 33: 6011–6016

Dinand E, Chanzy H, Vignon MR (1996) Parenchymal cell cellulose from sugar beet pulp: preparation and properties. Cellulose 3:183–188

Dinand E, Chanzy H, Vignon MR (1999) Suspensions of cellulose microfibrils from sugar beet pulp. Food Hydrocolloids 13:275–283

Doi M, Edwards SF (1986) The theory of polymer dynamics, Chapter 7. Oxford University Press, New York, pp 218–288

Fuller GD (1995) Optical rheometry of complex fluids. Oxford University Press, New York

Herrick FW, Casebier RL, Hamilton JK, Sandberg KR (1983) Microfibrillated cellulose; Morphology and accessibility. J Appl Polym Sci: Appl Polym Symp 37:797–813

Hioki N, Hori Y, Watanabe K, Morinaga Y, Yoshinaga F, Hibino Y, Ogura T (1995) Bacterial cellulose; as a new material for papermaking. Jpn Tappi J 49:82–87

Krishna Iyer K, Neelakantan P, Radhakrishnan T (1968) Birefringence of native cellulosic fibers. I. Untreated cotton and ramie. J Polym Sc A-2 6:1747–1758

Lepoutre P, Robertson AA (1974) Colloidal solutions from sodium polyacrylate-polyacrylamide grafted cellulose. TAPPI 57:87–90

Marchessault RH, Morehead FF, Joan Koch M (1961) Some hydrodynamic properties of neutral suspensions of cellulose crystallites as related to size and shape. J Colloid Sci 16:327–344

Nakagaito AN, Yano H (2004) The effect of morphological changes from pulp fiber towards nano-scale fibrillated cellulose on the mechanical properties of high-strength plant fiber based composites. Appl Phys A 78:547–552

Nakagaito AN, Yano H (2005) Novel high-strength biocomposites based on microfibrillated cellulose having nano-order-unit web-like network structure. Appl Phys A 80:155–159

Nishiyama Y, Kim UJ, Kim DY, Katsumata KS, May RP, Langan P (2003) Periodic disorder along ramie cellulose microfibrils. Biomacromolecules 4:1013–1017

Saito T, Nishiyama Y, Putaux J-L, Vignon MR, Isogai A (2006) Homogeneous suspensions of individualized microfibrils from TEMPO-catalyzed oxidation of native cellulose. Biomacromolecules 7:1687–1691

Saito T, Kimura S, Nishiyama Y, Isogai A (2007) Nanofibers prepared by TEMPO-mediated oxidation of native cellulose. Biomacromolecules 8:2485–2491

Turbak AF, Snyder FW, Sandberg KR (1983) Microfibrillated cellulose, a new cellulose product; properties, uses, and commercial potential. J Appl Polym Sci: Appl Polym Symp 37:815–827

Vian B, Reis D, Darzens D, Roland JC (1994) Cholesteric-like crystal analogs in glucuronoxylan-rich cell wall composites: experimental approach of acellular re-assembly from native cellulosic suspension. Protoplasma 180:70–81

Wiener O (1912) Die Theorie des mischkörpers für das Feld der stationären Strömung. Abh Math-Phys Klasse königlich sächischen Ges Wiss 32:509–604

Yano H, Sugiyama J, Nakagaito AN, Nogi M, Matsuura T, Hikita M, Handa K (2005) Optically transparent composites reinforced with networks of bacterial nanofibers. Adv Materials 17:153–155

Zimmermann T, Pöhler E, Geiger T (2004) Cellulose fibrils for polymer reinforcement. Adv Eng Mat 6(9):754–761